ANTIOXIDANTS & REDOX SIGNALING
Volume 18, Number 1, 2013

DOI: 10.1089/ars.2012.4584

Discoveries

ORIGINAL RESEARCH COMMUNICATION

A Role for Virally Induced Reactive Oxygen Species in Kaposi's Sarcoma Herpesvirus Tumorigenesis

Qi Ma,[1,2,*] Lucas E. Cavallin,[1,*] Howard J. Leung,[1] Chiara Chiozzini,[3,†] Pascal J. Goldschmidt-Clermont,[2] and Enrique A. Mesri[1]

Abstract

Aims: Kaposi's sarcoma (KS), caused by the Kaposi's sarcoma herpesvirus (KSHV), is an AIDS-associated cancer characterized by angiogenesis and proliferation of spindle cells. Rac1-activated reactive oxygen species (ROS) production has been implicated in KS tumorigenesis. We used an animal model of KSHV-induced Kaposi's sarcomagenesis (mECK36) to study the role of ROS in KS and the efficacy of N-acetyl L-cysteine (NAC) in inhibiting or preventing KS. ***Results:*** Signaling by the KSHV early lytic gene viral G protein-coupled receptor (vGPCR) activated ROS production in mECK36 cells *via* a Rac1-NADPH oxidase pathway. Induction of the lytic cycle in KSHV-infected KS spindle cells upregulated ROS along with upregulation of vGPCR expression. We also found that expression of the major latent transcript in 293 cells increased ROS levels. ROS scavenging with NAC halted mECK36 tumor growth in a KSHV-specific manner. NAC inhibited KSHV latent gene expression as well as tumor angiogenesis and lymphangiogenesis. These effects correlated with the reduction of vascular endothelial growth factor (VEGF), c-myc, and cyclin D1, and could be explained on the basis of inhibition of STAT3 tyrosine phosphorylation. NAC prevented mECK36 *de novo* tumor formation. Molecular analysis of NAC-resistant tumors revealed a strong upregulation of Rac1 and $p40^{PHOX}$. ***Innovation and Conclusion:*** Our results demonstrate that ROS-induction by KSHV plays a causal role in KS oncogenesis by promoting proliferation and angiogenesis. Our results show that both ROS and their molecular sources can be targeted therapeutically using NAC or other Food and Drug Administration (FDA)-approved inhibitors for prevention and treatment of AIDS-KS. *Antioxid. Redox Signal.* 18, 80–90.

Introduction

Reactive oxygen species (ROS) have an increasingly recognized broad function in oncogenesis (18, 19, 42, 44). One pathway responsible for ROS production is triggered by signaling cascades leading to Rac1 activation of NADPH-oxidases (NOX) family (7). ROS play a role in cell cycle regulation and angiogenesis, yet the specific molecular events linking ROS and these cancer hallmarks are still elusive (25, 43). Kaposi's sarcoma herpesvirus (KSHV, also called Human Herpes Virus 8) is the etiological agent of Kaposi's sarcoma (KS) (9, 14, 26). KS is a major cancer caused by KSHV, associated with HIV infection (AIDS-KS), and the most prevalent type of cancer affecting men and children in Sub-Saharan Africa (13, 15, 26, 37). KS is characterized by spindle cell proliferation, intense angiogenesis, and erythrocyte extravasation with variable inflammatory infiltrates (13, 15, 26, 37). Although the incidence of AIDS-KS in the Western world has

Innovation

Kaposi's sarcoma (KS) remains an incurable disease and preventive approaches are nonexistent. Here, we demonstrate that N-acetyl L-cysteine, a Food and Drug Administration-approved drug, effectively inhibits tumorigenesis in a Kaposi's sarcoma herpesvirus-driven KS mouse model. Our results suggest reactive oxygen species as therapeutic and chemopreventive targets for KS, providing opportunities for low cost drug development for KS treatment.

[1]Viral Oncology Program, Department of Microbiology and Immunology, Sylvester Comprehensive Cancer Center and Center for AIDS Research, University of Miami Miller School of Medicine, Miami, Florida.
[2]Department of Medicine, Vascular Biology Institute, University of Miami Miller School of Medicine, Miami, Florida.
[3]Weill Medical College of Cornell University, New York, New York.
*These two authors contributed equally to this work.
†*Current affiliation:* Istituto Superiore di Sanita, Rome, Italy.

declined, since the wide-spread implementation of Highly Active Antiretroviral Therapy, a significant percentage of AIDS-KS patients never achieve total remission (22, 32). Understanding the interplay of viral and host factors in KS carcinogenesis is critical for the rational development of new therapies (12, 41). KSHV-infected KS lesions are composed of latently infected cells and a rather small minority of cells expressing lytic genes, such as the angiogenic viral G protein-coupled receptor (vGPCR) (6, 20), which has been implicated in the development of KS angioproliferative phenotype *via* a paracrine mechanism (6, 8, 15, 26, 28). vGPCR is able to induce KS-like sarcomagenesis in transgenic mice (27, 47), and it is essential for KSHV tumor formation in mice in the KSHV-bearing tumor induced by mECK36 cells (30). The mECK36 cells are mouse bone marrow endothelial cells transfected with a KSHV bacterial artificial chromosome (30). mECK36 cells induce KS-like tumors in nude mice in a strict KSHV-dependent manner. These KS-like tumors, which have been validated as host and viral surrogates of KS, are suitable for testing anti-KS therapies as well as the role of viral genes in KS oncogenesis (30).

Rac1 is a critical mediator for vGPCR angiogenesis (29). We recently found that a constitutively activated Rac1 mutant induces KS-like tumors (24). We found that Rac1 is overexpressed in AIDS-KS lesions and in KSHV-infected mECK36 tumors, pointing to a role for KSHV-induced Rac1-mediated production of ROS in KS pathogenesis (24). Moreover, we found that the ROS scavenger N-acetyl L-cysteine (NAC) was able to completely suppress Rac1-induced tumor formation in RacCA transgenic mice, indicating a causal role of ROS in Rac-induced tumorigenesis (24). This finding, together with studies in KS spindle cell tumors (3), points to antioxidants such as NAC, a Food and Drug Administration (FDA)-approved drug, which has been shown to be safe and efficacious in increasing survival in HIV-infected patients (5, 17), as potential chemopreventive and therapeutic agents in KS. Before clinical implementation, the testing of antioxidants in models that accurately represent KSHV-infected KS lesions is required. In the present report, we show the chemopreventive and therapeutic activity of NAC in the mECK36 animal model of KSHV-induced KS tumorigenesis.

Results

KSHV-induced upregulation of oxidative stress and ROS production

We have previously shown that Rac1 is overexpressed in all spindle cells of KS lesions and in all KSHV-infected cells of mECK36 tumors (24, 30), suggesting that KSHV induction of oxidative signaling could play a role in KSHV oncogenesis. To establish a possible link between KSHV tumorigenesis and oxidative stress, we sought to identify whether KSHV genes could upregulate ROS production. To this end, since it has been established that vGPCR is a Rac1 activator, we first examined the production of ROS in mECK36 cells overexpressing vGPCR. We found that vGPCR overexpression with super activation by its ligand Gro-α led to superoxide production in a Rac1-dependent manner (Fig. 1A). Consistent with a ROS mechanism involving Rac1 activation of NOX, we found a much stronger inhibition of vGPCR-induced ROS production in the presence of the NOX inhibitor diphenylene

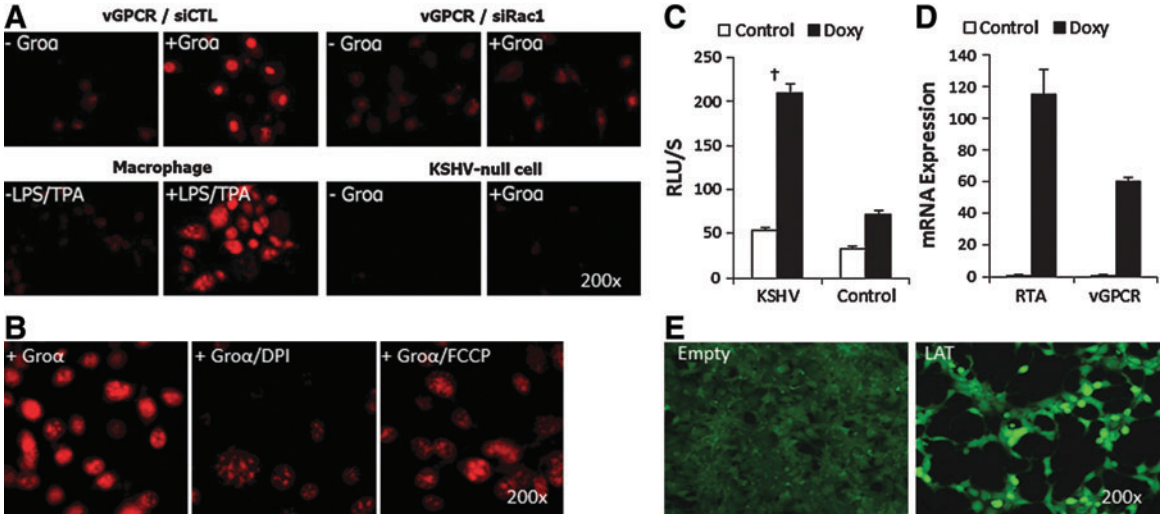

FIG. 1. vGPCR and LAT genes increase ROS production in a Rac1-dependent manner. (A) Superoxide production was measured by DHE staining in mECK36 cells transfected with a vGPCR-expressing plasmid and treated with siRac1 (Rac1 siRNA) or siCTL (control siRNA). LPS/TPA-stimulated macrophages were used as positive control. KSHV-null mECK36 cells, which do not express vGPCR, served as negative control. Groα is a vGPCR agonist. **(B)** Superoxide production of vGPCR-expressing mECK36 cells induced with Groα was measured by DHE staining using DPI or FCCP inhibitors. **(C)** ROS production measured by enhanced luminol assay in iSLK.219 cells upon stimulation with 0.5 μg/ml doxycyclin to induce lytic gene expression. **(D)** qRT-PCR analysis of KSHV lytic gene expression (RTA, vGPCR) in iSLK.219 cells upon stimulation with 0.5 μg/ml doxycyclin to induce lytic gene expression. Data indicate fold increase of mRNA as measured by duplicates in two independent experiments. **(E)** DCF staining of 293 cells either transfected with LAT vector expressing the major LAT encoding KSHV LANA, v-cyclin and vFLIP and control vector. $^{\dagger}p < 0.05$. DCF, 2′,7′-dichlorofluorescin; DHE, dihydroethidium; DPI, diphenylene iodonium; FCCP, *p*-(tri-fluromethoxy) phenyl-hydrazone; KSHV, Kaposi's sarcoma herpesvirus; LAT, latent transcript; LPS, lipopolysaccharide; qRT-PCR, quantitative real-time polymerase chain reaction; ROS, reactive oxygen species; RTA, replication transcriptional activator; TPA, 12-O-tetradecanoylphorbol-13-acetate; vGPCR, viral gene G protein-coupled receptor. (To see this illustration in color, the reader is referred to the web version of this article at www.liebertpub.com/ars.)

iodonium (DPI) than in the presence of the mitochondrial ROS inhibitor carbonyl cyanide *p*-(tri-fluromethoxy) phenylhydrazone (FCCP) (Fig. 1B). As vGPCR is a lytic gene, we then examined whether the induction of KSHV lytic cycle occurs with increased ROS production. Since many of the epigenetic drug inducers, such as TPA and butyrate, can themselves affect ROS production through indirect mechanisms, we resorted to the iSLK system (31), which is composed of KS spindle cells latently infected with rKSHV (iSLKr219) and its uninfected control. In these cells, lytic replication can be induced *via* tetracyclin-induced KSHV replication transcriptional activator expression. We found that induction of lytic replication in iSLKr219 cells occurred with a marked increase of ROS production along with a steep upregulation of vGPCR expression (Fig. 1C, D). Since explanted KS spindle cells, such as SLKs, have high levels of native oxidative stress (3), we used 293 cells to determine whether KSHV latent genes have the potential to induce ROS using a more stable ROS dye, 2′,7′-dichlorofluorescein diacetate (DCF-DA), that cannot be used in the context of the enhanced green fluorescent protein (eGFP) expressing mECK36 and iSLKs. We found that expression of the KSHV major latent transcript (LAT), which includes LANA, v-cyclin, and vFLIP, in 293 cells increased ROS production (Fig. 1E). Taken together, our results identify vGPCR activation of Rac1 and NOX as a key ROS-inducing pathway and show that both lytic and latent KSHV infection could be linked to oxidative stress production.

NAC inhibits KSHV-driven tumorigenesis by inhibition of angiogenesis, proliferation, and viral gene expression

Our results on KSHV-linked upregulation of ROS strongly point to the occurrence of ROS-mediated mechanisms in KSHV oncogenesis. To assess this possibility, we tested whether KSHV tumorigenesis could be prevented with the antioxidant NAC (24) using the mECK36 tumorigenesis model (30). To further establish a correlation between the occurrence *in vivo* of ROS-mediated oncogenic mechanisms and KSHV infection, we used a KSHV-negative (KSHV – ve) tumor that we established from explanted mECK36 tumor cells that had lost the KSHVBac36 episome by growth without antibiotic selection *in vitro* (30). In contrast to *in vitro* grown mECK36, in which loss of the episome leads to loss of tumorigenicity, cell populations that had become irreversibly transformed by KSHV during *in vivo* growth upon losing the KSHV Bac36 episome are able to generate KSHV-negative tumors in mice. We characterized one of these KSHV-negative mECK36 cell lines thoroughly for KSHV negativity by quantitative real-time polymerase chain reaction (qRT-PCR) and viral DNA PCR (see Materials and Methods). Genome-wide transcriptome analysis shows that KSHV-positive tumors share 81% of the human KS signature, while KSHV-negative tumors share 79% (Fig. 2A). This data indicates that KSHV-negative tumors belong to the same cell lineages as mECK36 tumors and share a significant overlap with the human KS transcriptome. Therefore, although the exact nature of the KSHV-independent oncogenic mechanisms of these cells remains to be established, they are the best available control to be used in combination with KSHV-positive mECK36 tumors, which are a model of KSHV-dependent tumorigenesis (30), to assess KSHV-specific biology. We found that, consistent with the data of Figure 1, KSHV-positive tumors were inhibited by NAC treatment (Fig. 2B), whereas KSHV-negative tumors were resistant to NAC antioxidant activity (Fig. 2C), indicating the involvement of a ROS-dependent mechanism in KSHV-induced tumorigenesis and pointing to ROS inhibition by antioxidants as a potential therapeutic approach for KS. To determine the molecular basis of NAC antitumor effect, we studied the level of expression of viral and host genes implicated in pathogenesis. LANA mRNA levels were downregulated together with the other genes of the major LAT v-cyclin and vFLIP in mECK36 tumors treated with NAC, whereas early lytic genes, such as vGPCR and vIL6, were either unaffected or upregulated by NAC (Fig. 3A). It is possible that activation of KSHV genes, such vIL-6, is part of a compensatory response to the antiangiogenic activities of NAC. Although these are believed to be pathogenic genes, the fact that NAC is antitumorigenic suggests that their pathogenic effect is overcome by the strong antitumor and antiangiogenic activity of NAC. To confirm these qRT-PCR results, we performed immunofluorescence staining of LANA on tumors treated for 3 days with NAC. We found that LANA protein levels were downregulated by NAC, whereas eGFP expression levels remained similar in both groups (Fig. 3B).

We recently found that Rac1-activated ROS could promote angiogenesis and vascular endothelial growth factor (VEGF) upregulation (24). Consistent with a role of ROS in KSHV angiogenesis, we found that NAC treatment significantly reduced levels of blood and lymphatic neovascularization as indicated by a decrease in CD31-positive and VEGF-R3-positive neovessels (Fig. 4C). This correlated with transcriptional inhibition of angiogenic growth factors that regulate microvessel proliferation and sprouting (VEGF-A) (10), VEGFR-2-mediated endothelial-specific signaling (ESM-1) (38, 40), and vessel maturation (Angpt-2) (Fig. 4A) (10). Importantly, none of these transcriptional effects of NAC were observed in KSHV-negative tumors in which NAC did not have antitumor activity (Fig. 4B).

To delve into transcriptional targets underpinning NAC anti-KSHV tumorigenic activity, we measured the impact of NAC on mRNA levels of c-myc, an oncogenic transcription factor that mediates ROS tumorigenesis (45). Figure 5 shows that NAC strongly reduced c-myc levels in KSHV-positive, but not in KSHV-negative tumors, indicating that ROS regulates c-myc transcription, as well as angiogenic transcription (Fig. 4A, B) in the context of KSHV oncogenesis. To show that NAC inhibition of c-myc has an impact in tumor cell cycle regulation, we determined the levels of the cell cycle G1/S transition protein Cyclin D1, which is a c-myc target gene, and found that it was downregulated upon NAC treatment *in vivo* (Fig. 5B).

ROS regulate oncogenic STAT3 transcription in KSHV tumorigenesis

STAT3 is a redox signaling transcription factor implicated in KS and KSHV infection (2, 4, 34, 49) that can mediate transcription of proliferative genes such as c-myc and angiogenic genes such as VEGF (50). To explore possible transcriptional targets of tumor inhibition by NAC, we analyzed the status of STAT3 activation. We found that NAC-treated tumors had a significant reduction of STAT3 Tyr705 phosphorylation (Fig. 5C), which would be consistent with the reduction of c-myc and VEGF levels. To be able to directly link c-myc and VEGF transcription in our cell and animal model of

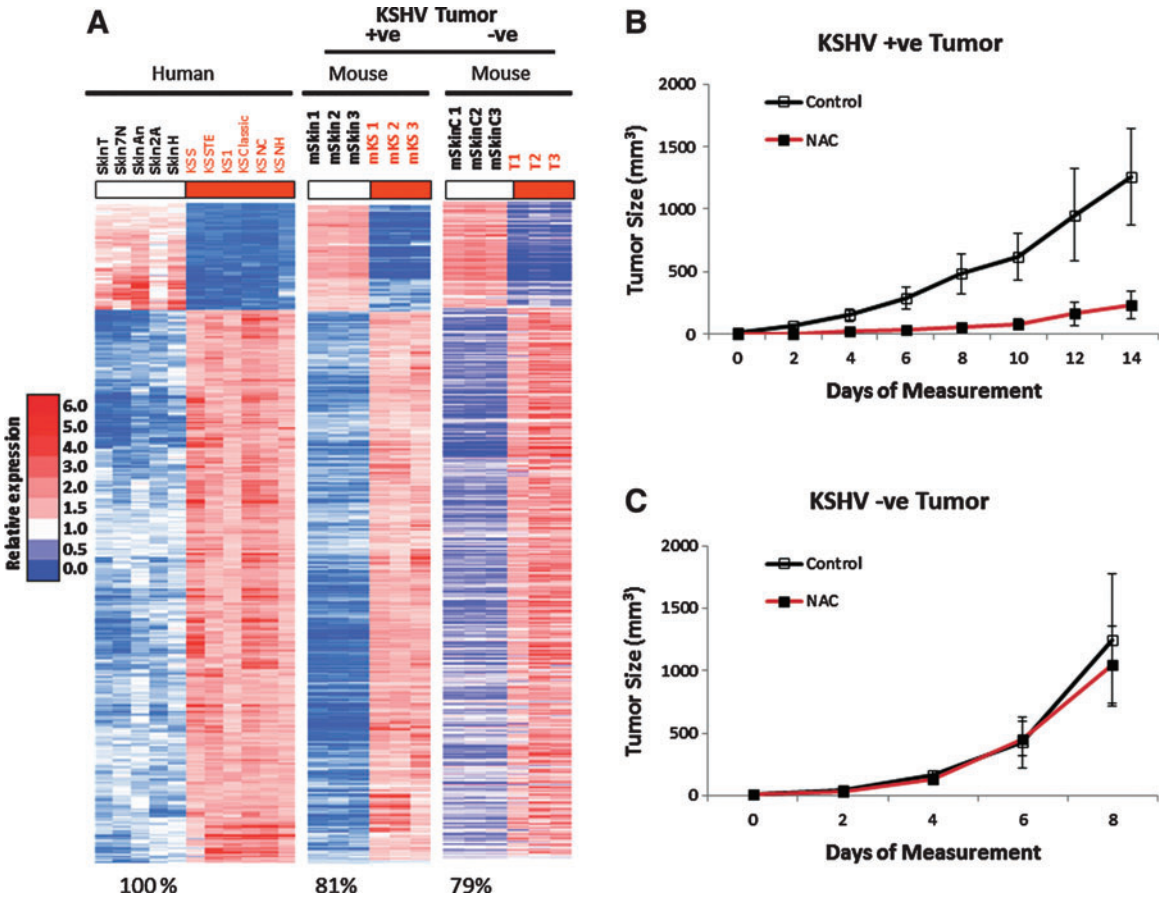

FIG. 2. NAC treatment inhibits KSHV-positive mECK36 tumor growth. (A) Validation of KSHV-negative mECK36 tumors by gene array signature analysis: Heat map representation of 562 genes ($q < 0.05$) of the human KS Signature that are also KSHV-positive mECK36 tumor signature (equally upregulated or downregulated) and KSHV − ve mouse signature. Seven hundred twenty-three genes from the human KS signature were orthologs to mouse genes present in the mouse Affymetrix Array. Among these, 691 genes were able to differentiate mECK36 spindle cell sarcomas and mouse skin ($q < 0.05$) for at least a two-fold difference. The figure shows genes that were upregulated (red) and downregulated (blue), respectively, in mECK36 tumors (KSHV + ve or KSHV − ve) and human KS. **(B, C)** Mice with established subcutaneous KSHV-positive (mECK36) tumors **(A**, $n = 7$**)** and KSHV-negative mECK36 tumors **(B**, $n = 5$**)** were treated with NAC (treatment modality). Animals received normal water (control) or water containing 40 m*M* NAC. Data indicate mean tumor size ± SD. Hollow bars indicate control tumors, solid bars indicate NAC-treated tumors. KS, Kaposi's sarcoma; NAC, N-acetyl L-cysteine; SD, standard deviation.

KS, we recreated the cytokine-rich environment of KS and mECK36 tumor by using an *in vitro* system of mECK36 cells stimulated with KS cytokines, which play key autocrine and paracrine roles in KS oncogenesis and are powerful ROS inducers. One of these paradigmatic KS cytokines is platelet-derived growth factor BB (PDGF-BB), an autocrine and paracrine KS growth factor overexpressed in KS lesions and in mECK36 tumors (26, 39) that can upregulate c-myc and VEGF through activation of platelet-derived growth factor receptor (PDGFR), a recently identified KS therapeutic target (21). We found that the KS cytokine PDGF-BB strongly stimulated STAT3 phosphorylation. STAT3 stimulation was abrogated

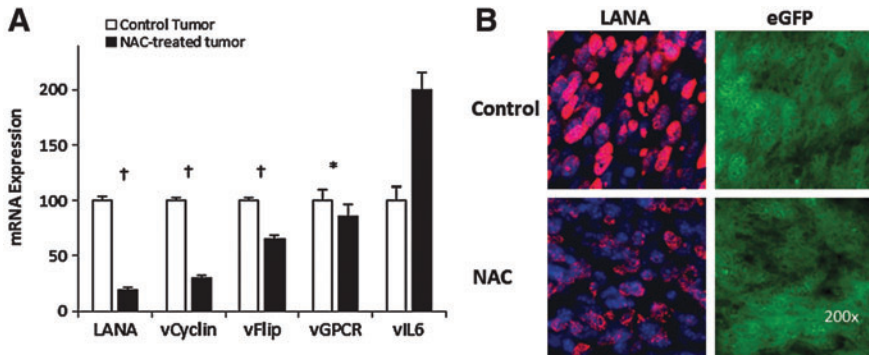

FIG. 3. NAC treatment inhibits KSHV gene expression genes in tumors. (A) Expression levels of LANA, vCyclin, vFlip, vGPCR, vIL6, and LANA in mECK36 tumors with and without NAC treatment were measured by RT-qPCR. Hollow bars indicate control tumors, solid bars indicate NAC-treated tumors. Significance was established by *t*-test: $^{*}p > 0.05$; $^{\dagger}p < 0.01$. **(B)** Change of LANA expression was examined in NAC-treated mECK36 tumors using immunofluorescence staining. RT-qPCR, real-time quantitative polymerase chain reaction.

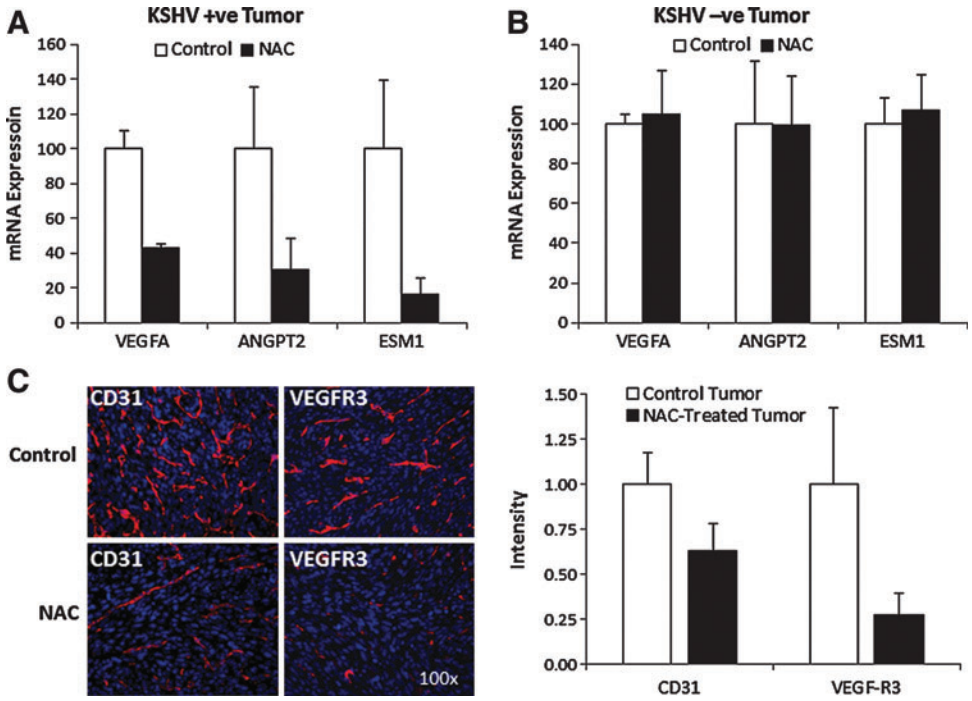

FIG. 4. NAC treatment affects host genes *in vivo*. (A, B) Expression levels of VEGF-A, Agpt2, and ESM1 in mECK36 tumors with and without NAC treatment were measured by RT-qPCR. **(C)** Immunostaining of NAC-treated and control mECK36 tumors stained with endothelial marker CD31 (red) and lymphatic marker VEGFR3 (red). Nuclei were counterstained with DAPI (blue). DAPI, 4′,6′-diamidino-2-phenylindole. (To see this illustration in color, the reader is referred to the web version of this article at www.liebertpub.com/ars.)

by NAC and by the Rac1 inhibitor EHT1864, indicating that PDGF stimulated STAT3 *via* a Rac1 and NOX-mediated pathway (Fig. 5D, E). Importantly, inhibition of STAT3 signaling using the JAK/STAT inhibitor AG490 led to a profound transcriptional inhibition of PDGF-BB-induced VEGF-A and c-myc upregulation, indicating that in the context of KSHV-infected cells stimulated by KS-cytokines, STAT3 is a ROS-dependent transcriptional regulator of c-myc and VEGF (Fig. 5F). Moreover, we found that the STAT3 inhibitor also inhibited LANA transcriptional levels. Our results suggest that the NAC antitumor effect is due in part to the targeting of STAT3-mediated transcription of c-myc, VEGF-A, and KSHV LANA in KSHV-positive tumors. This suggests that ROS are implicated in KSHV tumorigenesis by activating signaling cascades that regulate the phosphorylation of the ROS-dependent transcription factors, such as STAT3, which in turn could regulate host genes implicated in cell proliferation and angiogenesis as well as viral genes, such as LANA, implicated in episome retention. Taken together, these results support a mechanism whereby KSHV induces oxidative signaling to promote viral maintenance and oncogenesis, pointing to ROS as an attractive KS therapeutic target.

NAC treatment can prevent KSHV tumorigenesis

mECK36 cells growth in mice represent a model of *in vivo* inducible tumorigenesis (30). Therefore, we examined whether NAC could prevent the oncogenic process that mECK36 cells undergo *in vivo*. Mice were given NAC after receiving subcutaneous injections of either mECK36 cells or KSHV-negative cells. We found that mECK36 tumor formation was greatly inhibited with more than 2 weeks' delay in tumor onset time (Fig. 6A). Tumor formation of KSHV-negative mECK36 cells was unaffected by NAC treatment, indicating that NAC is targeting a specific KSHV-driven process (Fig. 6B). Since tumors that grew in a NAC treatment environment are to be considered NAC-resistant tumors, we examined changes on the levels of expression of oxidative stress and redox-related genes in an attempt to explore the mechanism of resistance. Interestingly, we found that $p40^{PHOX}$ and Rac1 were upregulated by an average of 22- and 47-fold, respectively (Fig. 6C), in NAC-resistant tumors. NOX2 and $p47^{PHOX}$ also showed significant upregulation. ROS-related gene upregulation in NAC-resistant tumors could either be the consequence of NAC-induced changes in gene expression or selection of resistant variants. To further characterize the selection mechanism, we analyzed the effects of NAC treatment on mECK36 tumors at 3, 7, and 14 days. As shown in Figure 6D, we could not detect significant effects of NAC on expression of NOX2, $p47^{PHOX}$, $p40^{PHOX}$, or Rac1. Hence, NAC-resistance is likely to be the consequence of NAC-induced selection of variants with increased expression of Rac1 and $p40^{PHOX}$. The fact that NAC selects for variants upregulating genes implicated in ROS production further underscores a causative role for ROS in KSHV tumorigenesis, reinforcing the concept of ROS as preventive and therapeutic targets in KS.

Discussion

Our results show that KSHV oncogenesis occurs through the KSHV gene-induced deregulation of ROS production. KSHV tumorigenesis is mediated by ROS-induced activation of angiogenesis and cell proliferation. Furthermore, targeting of ROS and ROS-mediated signaling is identified as a therapeutic or preventive approach in AIDS-KS.

Our data expand the role oxidative stress plays in KS pathogenesis from previous studies showing that antioxidants block KS spindle cell tumorigenicity to KSHV-dependent sarcomagenesis (3). This is consistent with Rac1 overexpression in all KSHV-infected cells of AIDS-KS lesions (24), which, together with upregulation of NOX members found in the KS molecular signature (46), are indicative of ongoing oxidative signaling. According to our results, ROS is increased in lytically infected cells and could be triggered by

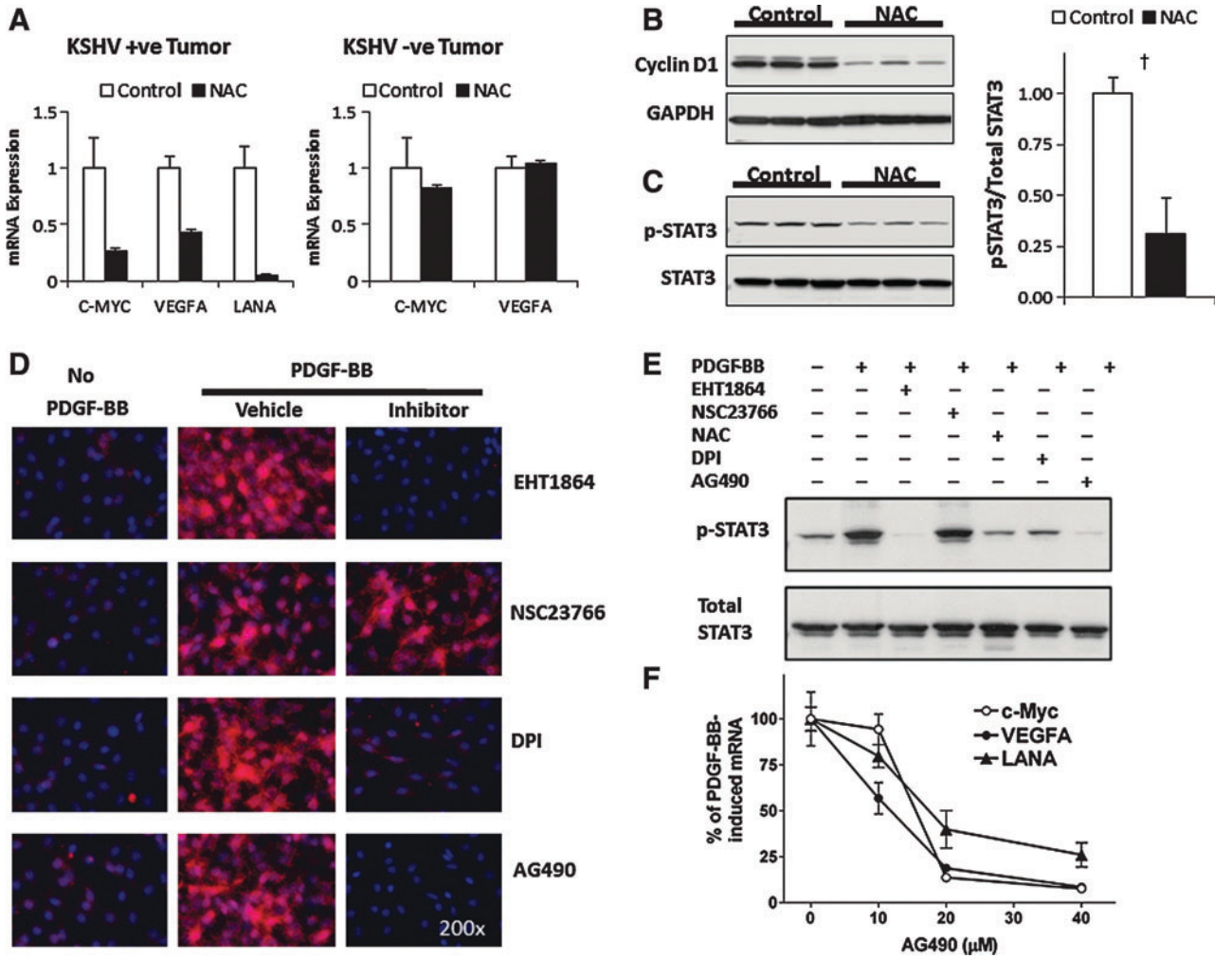

FIG. 5. ROS regulate oncogenic and angiogenic STAT3 transcription in KSHV tumorigenesis. (A) Expression levels of C-myc, VEGF-A, and LANA in mECK36 tumors with and without NAC treatment were measured by RT-qPCR. **(B, C)** Levels of Cyclin D1, p-STAT3 (Tyr705), and total STAT3 of NAC-treated and control tumors were determined by immunoblotting. Significance was established by *t*-test: $^{\dagger}p < 0.01$. **(D)** Immunostaining of serum-starved mECK36 cells stimulated with PDGF-BB (40 ng/ml) for 15 min. The following inhibitors were added 10 min before PDGF stimulation: EHT1864 (50 μM), NSC23766 (100 μM), NAC (40 mM), DPI (40 μM), and AG490 (30 μM). Red, phosphorylated STAT3. Blue (DAPI), nuclei. **(E)** Serum-starved mECK36 cells were treated with PDGF-BB (40 ng/ml) for 20 min. Cells were treated as in **(D)**. Levels of p-STAT3 (Tyr705) and total STAT3 were determined by immunoblotting. **(F)** Expression of c-Myc, VEGF-A, and LANA in serum-starved mECK36 cells stimulated with PDGF-BB in the presence or absence of increasing concentrations of Jak2 inhibitor AG490 was measured by RT-qPCR. PDGF-BB, platelet-derived growth factor BB. (To see this illustration in color, the reader is referred to the web version of this article at www.liebertpub.com/ars.)

vGPCR signaling *via* Rac1-mediated NOX activation. Our results with ROS increase during lytic replication are consistent with the ROS-producing role of the early lytic gene vGPCR, as well as with the upregulation of other KSHV lytic genes that are known to trigger signaling cascades that can activate oxidative stress, such as K1, K15, and vIL-6 (26). As lytic replication is considered essential for fueling the angiogenic and proliferative phenotype of KS lesions by promoting the secretion of cytokines, such as VEGF-A and PDGFB (26), our new data support that this mechanism could be mediated by ROS.

Our newly developed and validated KSHV-negative mECK36 tumor control shows that NAC inhibition of mECK36 is strictly KSHV-dependent. The KSHV-negative mECK36 tumor used as a control shared much of the molecular signature of KSHV-positive mECK36, and therefore it is a strong control for KSHV-specific mechanisms of tumorigenesis. In our previous study (30), we showed that KSHV-positive mECK36 tumorigenesis is reversible, *in vivo*-induced, and KSHV-dependent, since cultured mECK36 cells that have lost the virus were no longer able to form tumors. On the other hand, some explanted mECK36 cells from advanced tumors represent the irreversible KSHV-independent stage of tumorigenesis, since they do not lose tumorigenicity after losing the KSHV episome. The KSHV-negative mECK36 are representative of this stage. Thus, the data from both Figures 2 and 6 strongly indicate that KSHV tumorigenesis is ROS-dependent. This is consistent with our data on KSHV upregulation of ROS, suggesting a major role for ROS in tumorigenic mechanisms promoted by KSHV. NAC antitumor effects in mECK36 are consistent with our observations in our

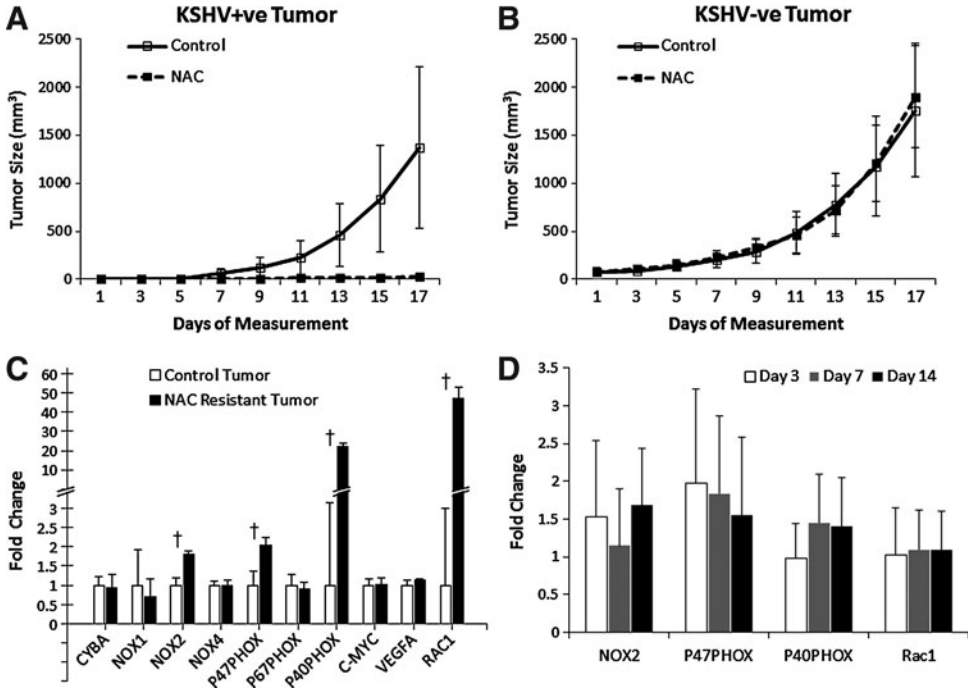

FIG. 6. NAC prevents KSHV-mediated tumorigenesis. (A, B) Mice were treated with NAC 2 weeks after injection of mECK36 cells ($n=7$) or KSHV-negative cells ($n=9$) (preventive modality). Animals received normal drinking water (control) or water containing 40 m*M* NAC. Data indicate mean tumor size ± SD. **(C, D)** Gene expression levels of a subset of viral, angiogenic, and redoxregulated genes were examined using RT-qPCR. Untreated mECK36 cells were used as controls. $^{\dagger}p<0.05$.

RacCA mouse model (24). NAC sensitivity was found to be KSHV-dependent. These results reinforce the idea that KSHV promotes oncogenic oxidative stress signaling, providing an explanation as to why KSHV-induced tumors are sensitive to NAC. We found that tumor growth inhibition induced by NAC correlated with downregulation of VEGF-A and c-myc in KSHV-infected tumors, while c-myc and VEGF levels were not affected in KSHV-negative tumors, suggesting that in the context of KSHV oncogenesis and KS, VEGF and c-myc are regulated by a ROS-sensitive transcriptional mechanism. Our results point to STAT3 as a one of the ROS-regulated transcription factors that are implicated in ROS-dependent VEGF and c-myc upregulation in KS. We found that NAC treatment led to a strong decrease in STAT3 phosphorylation. Furthermore, *in vitro* experiments where mECK36 cells are stimulated by cytokines overexpressed in mECK36 KS-like tumors indicate that STAT3 is a ROS-dependent regulator of c-myc, VEGF-A, and KSHV LANA.

The antiangiogenic and antilymphangiogenic response obtained with NAC further provides a strong rationale for its anti-KS tumor activity (1, 3). It was documented by staining of CD31 and VEGFR3 together with transcriptional analysis of angiogenic growth factors and signaling markers. Again, we found that this angiogenic marker inhibition by NAC occurred only in KSHV-infected tumors, indicating that KSHV-induced angiogenesis was regulated by ROS. The result is consistent with our finding showing that genetic silencing of the ROS-promoting vGPCR led to inhibition of angiogenesis and tumorigenesis in the mECK36 model (30).This is also consistent with a role of oxidative stress mechanism in the promotion of VEGF-mediated angiogenesis as we have previously described (24), with the HIF-1 inhibitory activity of antioxidants (16, 24), with our new finding showing that lytic gene expression upregulates ROS, and with our finding that vGPCR activates ROS *via* Rac1. These point to inhibition of oxidative signaling as a plausible anti-KS and KSHV-induced malignancies approach, which is consistent with recent studies in the KSHV-infected primary effusion lymphomas showing that ROS could play a role in KSHV lytic reactivation and lymphomagenesis both *in vitro* and *in vivo* (23, 48). Indeed, transcriptional analysis of NAC-treated tumors reveals a major variation in lytic viral gene expression with a clear tendency to inhibition by antioxidant treatment (data not shown). Our new results showing the upregulation of ROS by KSHV lytic reactivation suggest a reciprocal relationship between KSHV replication and ROS, which could be exploited for antiviral or antitumor purposes.

In the NAC prevention study, NAC greatly inhibited mECK36 tumor formation, presumably by negating the effects from KSHV-induced oncogenic oxidative stress. The selection of NAC-resistant cells could be considered as worrisome in the clinical setting. Yet, our model of prevention is limited by the fact that we are inoculating a heterogeneous tumor-causing mass of mECK36 cells into mice and we then measure the ability of NAC to tamper this effect. Considering NAC's preventive effect in the context of this very disadvantageous model, it is very conceivable that in the natural setting of rare cells being oncogenically transformed by the virus, clinically approved doses of NAC, such as the one that was previously employed in the HIV study and what we use would be a very effective treatment (36). Interestingly, in the case of the therapeutic modality, we did not find resistant tumors, since all tumors treated initially responded to NAC. The fact that NAC-resistant tumors from the prevention experiments upregulated NOX members, and Rac1 further suggests the existence of an underlying ROS-driven oncogenesis mechanism. The remarkable increase of Rac1 and PHOX expression in NAC-resistant tumors indicates that levels of expression of ROS-producing genes could determine resistance to antioxidants. It also suggests a critical role for Rac1 in KS oncogenesis, as previously demonstrated in our RacCA mouse model (24), further underscoring oxidative stress as a key chemoprevention target in KS. Interestingly, NAC, an FDA-approved drug indicated for several conditions

(5), has been shown to be safe and efficacious in increasing survival in HIV-infected patients (11, 17). It is tempting to speculate that NAC activity in increasing survivorship might be due to amelioration and/or prevention of AIDS-associated malignancies, such as KS. The inability of NAC to affect KSHV-negative KS may point to a limitation in treatment. However, in the current study, KSHV-negative KS is an artificially generated control and not a control representative of a clinical stage. In humans, all KS lesions, as mECK36 tumors, are infected with KSHV to a variable extent. The fact that mECK36 tumors, which as mentioned above do contain cells subpopulations that are irreversibly transformed by KSHV, respond to NAC treatment, points to a general response to NAC in naturally occurring KSHV-infected KS tumors. Our results warrant further clinical studies of NAC usage for KS prevention in KSHV + /HIV + populations, particularly in resource poor settings, such as Africa, where KS continues to be the major cancer affecting males and children (26).

In summary, our results highlight a ROS-dependent mechanism, whereby KSHV-induced ROS-regulated transcription induces growth and angiogenesis in infected cells. We propose that both ROS and their molecular sources could be targeted in a chemopreventive or therapeutic manner using NAC or other FDA-approved inhibitors. Our results warrant further preclinical studies and molecular exploration of ROS as a target for prevention and treatment of AIDS-KS.

Materials and Methods

Cell culture and reagents

mECK36 cells were obtained and cultured as previously described (30). KSHV-negative mECK36 were obtained from mECK36 tumor explants after Bac36 episome loss achieved by growth without hygromycin selection as previously described (30). KSHV-negative cells were further selected by weeding and cell sorting. Absence of KSHV genome was verified by PCR for LANA, K1, vIRF-1, ORF23, ORF 36, ORF 74, and K15. KSHV-negative mECK36 cell lineage of cells and tumors was verified by gene array (Fig. 2). HEK293T cells were cultured in the Dulbecco's modified Eagle medium (DMEM) with standard formulations. iSLK cells were obtained from the Ganem lab and cultured as previously described (31). Doxycycline was purchased from Clontech; NAC was from Sigma-Aldrich; and Groα from PeproTech. dihydroethidium (DHE) and 2′,7′-dichlorofluorescin (DCF) were purchased from Molecular Probes. Antibodies: p-STAT3 (Tyr705), STAT3, and GAPDH were purchased from Cell Signaling Technology; $p22^{PHOX}$, NOX2, and CyclinD1 from Santa Cruz Biotechnology, β-actin from Sigma-Aldrich, and LANA from Abcam.

Constructs

Rac1 siRNA was purchased from Dharmacon (Chicago, IL). Expression constructs: vGPCR was cloned into the pcDNA3 vector (Invitrogen) using *Eco*RI and *Xho*I restriction sites. The LAT transcript expression vector pBabe-LAT1 is composed of the pBabe backbone with an *Eco*RI-*Cla*I insertion of the KSHV latency locus, including its promoter (LANA-CYC-vFLIP).

ROS detection

DHE staining was adapted from Owusu-Ansah *et al.* (33). Briefly, serum-starved cells were incubated with DHE/Hank's Balanced Salt Solution (HBSS) at 10 μM for 30 min in a CO_2 incubator at 37°C (dark conditions), in the presence of growth factors and inhibitors if required. Cells were then washed three times with HBSS and images in the red channel were taken using a Zeiss ApoTome Axiovert 200M microscope.

DCF staining

Cells were seeded on chamber slides and serum-starved overnight. Cells were washed three times with HBSS and incubated with 20 μM of carboxy-H2DCFDA (Invitrogen Cat# C-400) in HBSS for 30 min in a CO_2 incubator at 37°C (dark conditions). Cells were then washed three times with HBSS and images in the green channel were taken using a Zeiss ApoTome Axiovert 200M microscope.

Enhanced luminol assay

A LumiMAX Superoxide Detection Kit (Agilent) was used to measure the superoxide production in iSLK cells. Briefly, iSLK.219 cells were cultured in standard conditions and induced by exposure to doxycycline. iSLK cells were used as control. Cells were trypsinized and allowed to recover in a suspension in normal media for 30 min in a CO_2 incubator at 37°C. 5×10^5 cells were resuspended in 100 μl SOA assay medium. Add 100 μl SOA assay medium–reagent mixture and incubate for 10 min at room temperature. Luminescence was measured in a Luminometer (Titertek-Berthold).

Array analysis of KSHV − ve cells

Using the Mouse Genome 430 2.0 Array (Affymetrix), we examined gene expression levels of three biological samples of KSHV + ve mECK36 and of KSHV − ve mECK36 tumors. RNA isolation (Trizol; Invitrogen), Turbo DNase treatment (Ambion), and RNA purification (RNAeasy; Qiagen) were done following the manufacturer's recommendations. The integrity of RNA was confirmed with a bioanalyzer (model 2100; Agilent Technologies). We synthesized, labeled, and hybridized cRNA onto arrays at Genome Explorations according to standard Affymetrix methods. Raw data intensity profiles were analyzed using the GeneSpring 7 (Agilent) to perform microarray normalization and statistical analysis. Statistically significant genes were selected by analysis of variance test to obtain the largest gene list that gave a false discovery rate of $<1\%$ (35). Significantly expressed genes were clustered with GeneSpring 7 (Agilent) using the Pearson correlation method. Mouse skin samples were obtained from gene expression omnibus (GEO) data sets GSM26945, GSM26946, and GSM26947.

Real-time quantitative polymerase chain reaction

RNA was isolated with the RNeasy Plus Kit (Qiagen) with on column DNase treatment. About 500 ng of RNA was transcribed into cDNA using Reverse Transcription System (Promega) according to manufacturer's instructions. Real-time quantitative polymerase chain reaction (RT-qPCR) was performed using an ABI Prism 7000 Sequence Detection System (Applied Biosystems) with SYBR Green PCR Master Mix (Quanta Biosciences). The following primer sets were used: GAPDH (5′-ACCCAGAAGACTGTGGATGG-3′, 5′-CACATT GGGGGTAGGAACAC-3′); LANA (5′-CCTGGAAGTCCCAC AGTGTT-3′, 5′-AGACACAGGATGGGATGGAG-3′); c-myc (5′-CAACGTCTTGGAACGTCAGA-3′, 5′-TCGTCTGCTTGA

ATGGACAG-3′); VEGF-A (5′-AGCACAGCAGATGTGAA TGC-3′, 5′-AATGCTTTCTCCGCTCTGAA-3′); CYBA (5′-TT GTTGCAGGAGTGCTCATC-3′, 5′-CACGGACAGCAGTAA GTGGA-3′); NOX1 (5′-CCGACAACAAGCTCAAAACA-3′, 5′-CCAGCCAGTGAGGAAGAGAC-3′); NOX2 (5′-CTTGCC ATCCATGGAGCTGAACG-3′, 5′-ACCACCTTGGTGATGA CCACC-3′); NOX4 (5′-CCAGAATGAGGATCCCAGAA-3′, 5′-ACCACCTGAAACATGCAACA-3′); $p47^{PHOX}$ (5′-GTCC CTGCATCCTATCTGGA-3′, 5′-ATGACCTCAATGGCTTC ACC-3′); $p67^{PHOX}$ (5′-GCAGTGGCCTACTTCCAGAG-3′, 5′-ACCTCACAGGCAAACAGCTT-3′); $p40^{PHOX}$ (5′-CAAA ACAAAAGGAGGGTCCA-3′, 5′-GTTTTGCGCCCATGTAG ACT-3′); and RAC1 (5′-CTGAAGTGCGACACCACTGTC-3′, 5′-CTTGAGTCCTCGCTGTGTGAG-3′). In every run, melting-curve analysis was performed to verify specificity of products as well as water and RT controls. Data were analyzed using the ΔΔCT method as previously described (30). Target gene expression was normalized to GAPDH by taking the difference between CT values for target genes and GAPDH (ΔCT value). These values were then calibrated to the control sample to give the ΔΔCT value. The fold target gene expression is given by the formula: $2^{\Delta\Delta CT}$.

Immunofluorescence staining

Immunostaining was performed as previously described (30). Briefly, cells and frozen sections from tumors were fixed in 4% paraformaldehyde for 10 min, washed with phosphate-buffered saline (PBS), and permeabilized in 0.2% Triton-X/PBS for 20 min at 4°C. After blocking with 10% fetal bovine serum/PBS for 60 min, samples were incubated with anti-phospho STAT3, anti-LANA, anti-$p22^{PHOX}$, anti-NOX2, anti-CD31, and anti-VEGFR3 antibodies (1:200 dilutions) for 1 h. After PBS washing, samples were incubated with the secondary antibody Alexa Fluor 555 for 1 h (1:500 dilution; Molecular Probes), washed, and mounted with ProLong® Gold antifade reagent with 4′,6′-diamidino-2-phenylindole (Molecular Probes). Images were taken using a Zeiss ApoTome Axiovert 200M microscope. Image quantification was performed with ImageJ (NIH).

Western blotting

Protein concentrations in cell and tumor lysates were quantified using the DC Protein Assay (Bio-Rad). Twenty micrograms of protein was mixed with the Laemmli buffer, boiled for 5 min, resolved by sodium dodecyl sulfate–polyacrylamide gel electrophoresis, and transferred to polyvinylidene fluoride (PVDF) membranes (Bio-Rad Laboratories). Membranes were blocked with 5% nonfat milk/PBS for 1 h and incubated with primary antibodies (4°C, 16 h). After three Tris-buffered saline with Tween 20 (TBS/T) washes, membranes were incubated with horseradish peroxidase-labeled secondary antibodies (1:10,000 dilution; Promega) for 1 h at room temperature. Protein bands were developed using ECL Plus Detection Reagents (GE Healthcare) and quantified by densitometry with QuantityOne software (Bio-Rad Laboratories). To analyze multiple proteins on the same membrane, membranes were washed with the Restore PLUS Western Blot Stripping Buffer (Thermo Scientific) according to manufacturer's protocol.

Animal studies

All mice were housed under pathogen-free conditions. The animal studies were performed according to the protocols approved by the Institutional Animal Care and Use Committee at the University of Miami. Tumor studies were done in 4- to 6-week-old male Athymic Nude mice obtained from the National Cancer Institute. Tumors were generated by subcutaneous injection of either mECK36 cells (3×10^5 cells) or KSHV-negative cells (3×10^5 cells) as previously described (30). A group of mice was treated with 40 m*M* NAC in drinking water 2 weeks after tumor inoculation (preventive modality) or when tumors were already established and became visible (treatment modality) (24). This NAC regimen assumes that the steady-state concentration of NAC is 9.2 m*M* or 1.5 g/l NAC for a 20 g mouse (16). The control group received regular drinking water without NAC. Tumor volumes were measured using a caliber every 2 days and calculated using the following formula: [length (mm) × width $(mm)^2\times0.52$].

Statistical analysis

Statistical significance of the data was determined using the two-tailed Student's *t*-test. *p*-value lower than 0.05 was considered significant. Statistical analysis was performed using Unistat Statistical Package for Microsoft Excel. All values are expressed as means ± standard deviation.

Accession numbers

Details of quality control measures and all microarray data can be accessed from NCBI's GEO with accession number GSE6482.

Acknowledgments

We thank Brittany Ashlock and E.M. Duran for technical support and advice. Dr. S.-J. Gao for providing reagents and Dr. George McNamara from the Imaging and Molecular core facility (DRI, University of Miami). We thank Dr. Stephan Schurer for analyzing published kinase activity data for this study. We acknowledge resources of the Center of Computational Science at the University of Miami. This work was supported by NIH grants CA75918 (to E.A.M.), HL71536 (to P.J.G.), CA136387 (to E.A.M. and P.J.G.), and by NCI/OHAM supplements to the Developmental Center for AIDS Research grant 5P30AI073961.

Author Disclosure Statement

The authors declare no competing financial interests.

References

1. Agarwal A, Munoz-Najar U, Klueh U, Shih SC, and Claffey KP. N-acetyl-cysteine promotes angiostatin production and vascular collapse in an orthotopic model of breast cancer. *Am J Pathol* 164: 1683–1696, 2004.
2. Akira S, Nishio Y, Inoue M, Wang XJ, Wei S, Matsusaka T, Yoshida K, Sudo T, Naruto M, and Kishimoto T. Molecular cloning of APRF, a novel IFN-stimulated gene factor 3 p91-related transcription factor involved in the gp130-mediated signaling pathway. *Cell* 77: 63–71, 1994.
3. Albini A, Morini M, D'Agostini F, Ferrari N, Campelli F, Arena G, Noonan DM, Pesce C, and De Flora S. Inhibition of angiogenesis-driven Kaposi's sarcoma tumor growth in nude mice by oral N-acetylcysteine. *Cancer Res* 61: 8171–8178, 2001.

4. Aoki Y, Feldman GM, and Tosato G. Inhibition of STAT3 signaling induces apoptosis and decreases survivin expression in primary effusion lymphoma. *Blood* 101: 1535–1542, 2003.
5. Atkuri KR, Mantovani JJ, Herzenberg LA, and Herzenberg LA. N-acetylcysteine—a safe antidote for cysteine/glutathione deficiency. *Curr Opin Pharmacol* 7: 355–359, 2007.
6. Bais C, Santomasso B, Coso O, Arvanitakis L, Raaka EG, Gutkind JS, Asch AS, Cesarman E, Gershengorn MC, and Mesri EA. G-protein-coupled receptor of Kaposi's sarcoma-associated herpesvirus is a viral oncogene and angiogenesis activator. *Nature* 391: 86–89, 1998.
7. Bedard K and Krause KH. The NOX family of ROS-generating NADPH oxidases: physiology and pathophysiology. *Physiol Rev* 87: 245–313, 2007.
8. Cesarman E, Mesri EA, and Gershengorn MC. Viral G protein-coupled receptor and Kaposi's sarcoma: a model of paracrine neoplasia? *J Exp Med* 191: 417–422, 2000.
9. Chang Y, Cesarman E, Pessin MS, Lee F, Culpepper J, Knowles DM, and Moore PS. Identification of herpesvirus-like DNA sequences in AIDS-associated Kaposi's sarcoma. *Science* 266: 1865–1869, 1994.
10. Chung AS and Ferrara N. Developmental and pathological angiogenesis. *Annu Rev Cell Dev Biol* 27: 563–584, 2011.
11. De Rosa SC, Zaretsky MD, Dubs JG, Roederer M, Anderson M, Green A, Mitra D, Watanabe N, Nakamura H, Tjioe I, Deresinski SC, Moore WA, Ela SW, Parks D, Herzenberg LA, and Herzenberg LA. N-acetylcysteine replenishes glutathione in HIV infection. *Eur J Clin Invest* 30: 915–929, 2000.
12. Dittmer DP and Krown SE. Targeted therapy for Kaposi's sarcoma and Kaposi's sarcoma-associated herpesvirus. *Curr Opin Oncol* 19: 452–457, 2007.
13. Gallo RC. The enigmas of Kaposi's sarcoma. *Science* 282: 1837–1839, 1998.
14. Ganem D. KSHV infection and the pathogenesis of Kaposi's sarcoma. *Annu Rev Pathol* 1: 273–296, 2006.
15. Ganem D. KSHV and the pathogenesis of Kaposi sarcoma: listening to human biology and medicine. *J Clin Invest* 120: 939–949, 2010.
16. Gao P, Zhang H, Dinavahi R, Li F, Xiang Y, Raman V, Bhujwalla ZM, Felsher DW, Cheng L, Pevsner J, Lee LA, Semenza GL, and Dang CV. HIF-dependent antitumorigenic effect of antioxidants *in vivo*. *Cancer Cell* 12: 230–238, 2007.
17. Herzenberg LA, De Rosa SC, Dubs JG, Roederer M, Anderson MT, Ela SW, Deresinski SC, and Herzenberg LA. Glutathione deficiency is associated with impaired survival in HIV disease. *Proc Natl Acad Sci U S A* 94: 1967–1972, 1997.
18. Hussain SP, Hofseth LJ, and Harris CC. Radical causes of cancer. *Nat Rev Cancer* 3: 276–285, 2003.
19. Irani K, Xia Y, Zweier JL, Sollott SJ, Der CJ, Fearon ER, Sundaresan M, Finkel T, and Goldschmidt-Clermont PJ. Mitogenic signaling mediated by oxidants in Ras-transformed fibroblasts. *Science* 275: 1649–1652, 1997.
20. Kirshner JR, Staskus K, Haase A, Lagunoff M, and Ganem D. Expression of the open reading frame 74 (G-protein-coupled receptor) gene of Kaposi's sarcoma (KS)-associated herpesvirus: implications for KS pathogenesis. *J Virol* 73: 6006–6014, 1999.
21. Koon HB, Bubley GJ, Pantanowitz L, Masiello D, Smith B, Crosby K, Proper J, Weeden W, Miller TE, Chatis P, Egorin MJ, Tahan SR, and Dezube BJ. Imatinib-induced regression of AIDS-related Kaposi's sarcoma. *J Clin Oncol* 23: 982–989, 2005.
22. Krown SE. Therapy of AIDS-associated Kaposi's sarcoma: targeting pathogenetic mechanisms. *Hematol Oncol Clin North Am* 17: 763–783, 2003.
23. Li X, Feng J, and Sun R. Oxidative stress induces reactivation of Kaposi's sarcoma-associated herpesvirus and death of primary effusion lymphoma cells. *J Virol* 85: 715–724, 2011.
24. Ma Q, Cavallin LE, Yan B, Zhu S, Duran EM, Wang H, Hale LP, Dong C, Cesarman E, Mesri EA, and Goldschmidt-Clermont PJ. Antitumorigenesis of antioxidants in a transgenic Rac1 model of Kaposi's sarcoma. *Proc Natl Acad Sci U S A* 106: 8683–8688, 2009.
25. Menon SG, Sarsour EH, Kalen AL, Venkataraman S, Hitchler MJ, Domann FE, Oberley LW, and Goswami PC. Superoxide signaling mediates N-acetyl-L-cysteine-induced G1 arrest: regulatory role of cyclin D1 and manganese superoxide dismutase. *Cancer Res* 67: 6392–6399, 2007.
26. Mesri EA, Cesarman E, and Boshoff C. Kaposi's sarcoma and its associated herpesvirus. *Nat Rev Cancer* 10: 707–719, 2010.
27. Montaner S, Sodhi A, Molinolo A, Bugge TH, Sawai ET, He Y, Li Y, Ray PE, and Gutkind JS. Endothelial infection with KSHV genes *in vivo* reveals that vGPCR initiates Kaposi's sarcomagenesis and can promote the tumorigenic potential of viral latent genes. *Cancer Cell* 3: 23–36, 2003.
28. Montaner S, Sodhi A, Ramsdell AK, Martin D, Hu J, Sawai ET, and Gutkind JS. The Kaposi's sarcoma-associated herpesvirus G protein-coupled receptor as a therapeutic target for the treatment of Kaposi's sarcoma. *Cancer Res* 66: 168–174, 2006.
29. Montaner S, Sodhi A, Servitja JM, Ramsdell AK, Barac A, Sawai ET, and Gutkind JS. The small GTPase Rac1 links the Kaposi sarcoma-associated herpesvirus vGPCR to cytokine secretion and paracrine neoplasia. *Blood* 104: 2903–2911, 2004.
30. Mutlu AD, Cavallin LE, Vincent L, Chiozzini C, Eroles P, Duran EM, Asgari Z, Hooper AT, La Perle KM, Hilsher C, Gao SJ, Dittmer DP, Rafii S, and Mesri EA. *In vivo*-restricted and reversible malignancy induced by human herpesvirus-8 KSHV: a cell and animal model of virally induced Kaposi's sarcoma. *Cancer Cell* 11: 245–258, 2007.
31. Myoung J and Ganem D. Generation of a doxycycline-inducible KSHV producer cell line of endothelial origin: maintenance of tight latency with efficient reactivation upon induction. *J Virol Methods* 174: 12–21, 2011.
32. Nguyen HQ, Magaret AS, Kitahata MM, Van Rompaey SE, Wald A, and Casper C. Persistent Kaposi sarcoma in the era of highly active antiretroviral therapy: characterizing the predictors of clinical response. *Aids* 22: 937–945, 2008.
33. Owusu-Ansah E, Yavari A, Mandal S, and Banerjee U. Distinct mitochondrial retrograde signals control the G1-S cell cycle checkpoint. *Nat Genet* 40: 356–361, 2008.
34. Punjabi AS, Carroll PA, Chen L, and Lagunoff M. Persistent activation of STAT3 by latent Kaposi's sarcoma-associated herpesvirus infection of endothelial cells. *J Virol* 81: 2449–2458, 2007.
35. Reiner A, Yekutieli D, and Benjamini Y. Identifying differentially expressed genes using false discovery rate controlling procedures. *Bioinformatics* 19: 368–375, 2003.
36. Roederer M, Staal FJ, Raju PA, Ela SW, Herzenberg LA, and Herzenberg LA. Cytokine-stimulated human immunodeficiency virus replication is inhibited by N-acetyl-L-cysteine. *Proc Natl Acad Sci U S A* 87: 4884–4888, 1990.
37. Safai B, Johnson KG, Myskowski PL, Koziner B, Yang SY, Cunningham-Rundles S, Godbold JH, and Dupont B. The natural history of Kaposi's sarcoma in the acquired immunodeficiency syndrome. *Ann Intern Med* 103: 744–750, 1985.

38. Sarrazin S, Adam E, Lyon M, Depontieu F, Motte V, Landolfi C, Lortat-Jacob H, Bechard D, Lassalle P, and Delehedde M. Endocan or endothelial cell specific molecule-1 (ESM-1): a potential novel endothelial cell marker and a new target for cancer therapy. *Biochim Biophys Acta* 1765: 25–37, 2006.
39. Sharma-Walia N, Paul AG, Bottero V, Sadagopan S, Veettil MV, Kerur N, and Chandran B. Kaposi's sarcoma associated herpes virus (KSHV) induced COX-2: a key factor in latency, inflammation, angiogenesis, cell survival and invasion. *PLoS Pathog* 6: e1000777, 2010.
40. Shin JW, Huggenberger R, and Detmar M. Transcriptional profiling of VEGF-A and VEGF-C target genes in lymphatic endothelium reveals endothelial-specific molecule-1 as a novel mediator of lymphangiogenesis. *Blood* 112: 2318–2326, 2008.
41. Sullivan RJ, Pantanowitz L, and Dezube BJ. Targeted therapy for Kaposi sarcoma. *BioDrugs* 23: 69–75, 2009.
42. Szatrowski TP and Nathan CF. Production of large amounts of hydrogen peroxide by human tumor cells. *Cancer Res* 51: 794–798, 1991.
43. Ushio-Fukai M. Redox signaling in angiogenesis: role of NADPH oxidase. *Cardiovasc Res* 71: 226–235, 2006.
44. Ushio-Fukai M and Alexander RW. Reactive oxygen species as mediators of angiogenesis signaling: role of NAD(P)H oxidase. *Mol Cell Biochem* 264: 85–97, 2004.
45. Wade M and Wahl GM. c-Myc, genome instability, and tumorigenesis: the devil is in the details. *Curr Top Microbiol Immunol* 302: 169–203, 2006.
46. Wang HW, Trotter MW, Lagos D, Bourboulia D, Henderson S, Makinen T, Elliman S, Flanagan AM, Alitalo K, and Boshoff C. Kaposi sarcoma herpesvirus-induced cellular reprogramming contributes to the lymphatic endothelial gene expression in Kaposi sarcoma. *Nat Genet* 36: 687–693, 2004.
47. Yang TY, Chen SC, Leach MW, Manfra D, Homey B, Wiekowski M, Sullivan L, Jenh CH, Narula SK, Chensue SW, and Lira SA. Transgenic expression of the chemokine receptor encoded by human herpesvirus 8 induces an angioproliferative disease resembling Kaposi's sarcoma. *J Exp Med* 191: 445–454, 2000.
48. Ye F, Zhou F, Bedolla RG, Jones T, Lei X, Kang T, Guadalupe M, and Gao SJ. Reactive oxygen species hydrogen peroxide mediates Kaposi's sarcoma-associated herpesvirus reactivation from latency. *PLoS Pathog* 7: e1002054, 2011.
49. Yoon S, Woo SU, Kang JH, Kim K, Kwon MH, Park S, Shin HJ, Gwak HS, and Chwae YJ. STAT3 transcriptional factor activated by reactive oxygen species induces IL6 in starvation-induced autophagy of cancer cells. *Autophagy* 6: 1125–1138, 2010.
50. Yu H and Jove R. The STATs of cancer—new molecular targets come of age. *Nat Rev Cancer* 4: 97–105, 2004.

Address correspondence to:
Dr. Pascal J. Goldschmidt-Clermont
Department of Medicine
Vascular Biology Institute
University of Miami Miller School of Medicine
Miami, FL 33136

E-mail: pgoldschmidt@med.miami.edu

Dr. Enrique A. Mesri
Department of Microbiology and Immunology
Sylvester Cancer Center
University of Miami Miller School of Medicine
1550 NW 10th Ave.
Papanicolau Bldg, Room 109B
Miami, FL 33136

E-mail: emesri@med.miami.edu

Date of first submission to ARS Central, February 26, 2012; date of final revised submission, June 20, 2012; date of acceptance, July 1, 2012.

Abbreviations Used

DAPI = 4′,6′-diamidino-2-phenylindole
DCF = 2′,7′-dichlorofluorescin
DHE = dihydroethidium
DPI = diphenylene iodonium
eGFP = enhanced green fluorescent protein
FDA = Food and Drug Administration
GEO = gene expression omnibus
HBSS = Hank's Balanced Salt Solution
KS = Kaposi's sarcoma
KSHV = Kaposi's sarcoma herpesvirus
LAT = latent transcript
LPS = lipopolysaccharide
NAC = N-acetyle L-cysteine
NOX = NADPH-oxidases
PBS = phosphate-buffered saline
PDGF-BB = platelet-derived growth factor BB
ROS = reactive oxygen species
RT-qPCR = real-time quantitative polymerase chain reaction
SD = standard deviation
TPA = 12-O-tetradecanoylphorbol-13-acetate
VEGF = vascular endothelial growth factor
vGPCR = viral gene G protein-coupled receptor